METAL-FREE ELECTROCHEMICAL CATALYSTS FOR OXYGEN REDUCTION REACTION

*Y. Zheng, J. Liang, Q. H. Hu, S. Z. Qiao**

ARC Centre of Excellence for Functional Nanomaterials, Australian Institute for Bioengineering and Nanotechnology, The University of Queensland, QLD 4072, Australia. Email: s.qiao@uq.edu.au

Introduction

Although precious Pt has been adopted as an effective oxygen reduction reaction (ORR) electrocatalyst, large-scale commercial production has been restricted by its prohibitive cost, limited supply, and weak durability. The state-of-the-art metal-free nitrogen-doped carbon (N-carbon) materials are generally accepted as a potential substitute for Pt to reduce the cost, enhance the stability of ORR electrocatalysts and then promote the commercialization of fuel cell technology. However, the relatively low nitrogen content (2-5%) and a leaching of nitrogen active sites result in low and unstable catalytic activity of N-carbon materials.

Graphitic carbon nitride, referred to as g-C_3N_4, can be synthesized from a simple precursor via a series of polycondensation reactions without any metal involvement. g-C_3N_4 shows remarkably high catalytic activity for a variety of reactions such as photocatalytic hydrogen production.[1,2] Because of its high nitrogen content and facile synthesis procedure, g-C_3N_4 may provide more active reaction sites than other N-carbon materials to serve as a feasible metal-free ORR electrocatalyst. However, reports on the application of g-C_3N_4 in fuel cells and other electrochemical applications are rare.[3]

Herein we incorporate g-C_3N_4 catalyst into the framework of a highly ordered mesoporous carbon as a g-C_3N_4@carbon to promote electron transfer in the composite and increase the concentration of active sites facilitating ORR. Consequently, the nanoporous g-C_3N_4@carbon showed an excellent electrocatalytic ORR activity and perfect (nearly 100%) four-electron (4e–) ORR pathway selectivity in alkaline aqueous solution. Furthermore, the newly developed catalyst also revealed a remarkable methanol tolerance thus avoiding cross-over effects. To the best of our knowledge, such excellent electrochemical performance, which is competitive to commercial Pt/C catalyst, has been rarely observed for metal-free materials.[4]

Experimental

Nanoporous g-C_3N_4@CMK-3 composite was synthesized by a nanocasting method. Typically, 0.1 g fresh CMK-3 powders were dispersed in concentrated HNO_3 (10 mL, 70 %, Aldrich) for 5 hours at 50 °C to induce hydrophilicity. After washed by water until neutral and dried at 100 °C for overnight, 0.25 g of 50 wt% cyanamide ($CN-NH_2$, 99 %, Aldrich) aqueous solution and 0.25 g water were added. The mixture was stirred overnight and dried statically at 30 °C in the air for 24 h. The dried powder was calcined at 550 °C for 4 h in an Ar atmosphere with a heating rate of 4 °C/min to get the final g-C_3N_4@CMK-3 product.

Results and Discussion

High-resolution transmission electron microscopy (HRTEM) images of the g-C_3N_4@CMK-3 composite (Figure 1a and 1b inset) confirm its highly ordered mesoporous structure. The hexagonal pattern of the *P6mm* symmetrical mesoporous structure can be explicitly observed in Figure 1a and 1b, indicating a homogeneous distribution of g-C_3N_4 in the framework of CMK-3. As shown in Figure 1c, g-C_3N_4@CMK-3 reveals a similar shape of the nitrogen sorption isotherm (type IV with a distinct hysteresis loop) as CMK-3 (not shown here), indicating that the addition of g-C_3N_4 did not cause a significant deterioration of the structure of CMK-3. The obvious decrease in both surface area and pore volume confirms the mesopore filling effect during the impregnation process. After impregnation with g-C_3N_4, the original (110) and (200) diffraction peaks on the XRD pattern of CMK-3 almost disappear because of the mesopore filling by g-C_3N_4 (Figure 1d). The smaller primary pore size of g-C_3N_4@CMK-3 compared to pristine CMK-3, and the narrow pore size distribution (inset of Figure 1c) indicate that the *in-situ* synthesized g-C_3N_4 is almost homogeneously distributed on the surface of carbon nanorods, as illustrated by the inset of Figure 1a, resulting in the pore size reduction.

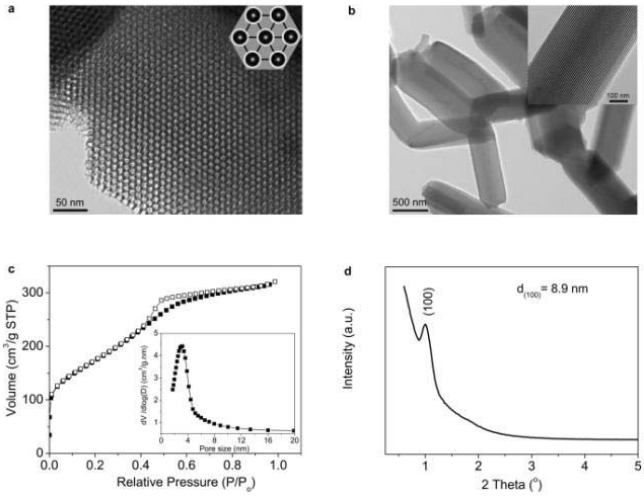

Figure 1. (a,b) Typical HRTEM images of ordered mesoporous g-C_3N_4@CMK-3 nanorods. Inset in panel a represents a schematic illustration (yellow: g-C_3N_4, black: carbon); inset in panel b reveals the ordered mesoporous channels. (c) Nitrogen sorption isotherm at 77 K with the corresponding pore size distribution (inset) and (d) low-angle XRD pattern of g-C_3N_4@CMK-3.

The electrocatalytic activities for ORR on g-C_3N_4@CMK-3 composite and pristine mesoporous g-C_3N_4 (denoted as g-C_3N_4(m), prepared using mesoporous silica SBA-15 as a sacrificial template) were first examined by cyclic voltammograms (CVs) in O_2-saturated 0.1 M KOH aqueous solution. A physical mixture of CMK-3 and g-C_3N_4(m) (denoted as mixed g-C_3N_4+CMK-3) with identical catalyst content as *in-situ* synthesized g-C_3N_4@CMK-3 was also prepared to investigate the possible nanoconfinement phenomena of g-C_3N_4@CMK-3. As shown in Figure 2a, the CV curve recorded for g-C_3N_4@CMK-3 is similar to those obtained on other carbon-based metal-free electrocatalysts with a single ORR peak at -0.25 V.[3, 5, 6] Compared with g-C_3N_4(m) and mixed g-C_3N_4+CMK-3, the g-C_3N_4@CMK-3 electrode revealed a more obvious ORR peak with a larger cathodic current, indicating a better electrocatalytic performance for ORR.

A series of linear sweep voltammograms (LSV) on rotating disk electrode (RDE) further revealed the lower onset potential and higher ORR current density on g-C_3N_4@CMK-3 than g-C_3N_4(m) and mixed g-C_3N_4+CMK-3 electrodes (Figure 2b). Besides, the onset potential on g-C_3N_4@CMK-3 is only ~0.1 V more negative than that on commercial Pt/C catalyst. At -0.6 V, g-C_3N_4@CMK-3 shows a comparable ORR current density with that observed on Pt/C. It should be noted that the LSV obtained on g-C_3N_4(m) shows a reduction peak at -0.49V without a current plateau, indicating a $2e^-$ ORR process from O_2 to OOH^- under this voltage. In contrast, the

Proceedings Published 2012 by the American Chemical Society

wide current plateau on g-C_3N_4@CMK-3 is considered as the strong limiting diffusion current, indicating a diffusion-controlled process related to an efficient $4e^-$ dominated ORR pathway.

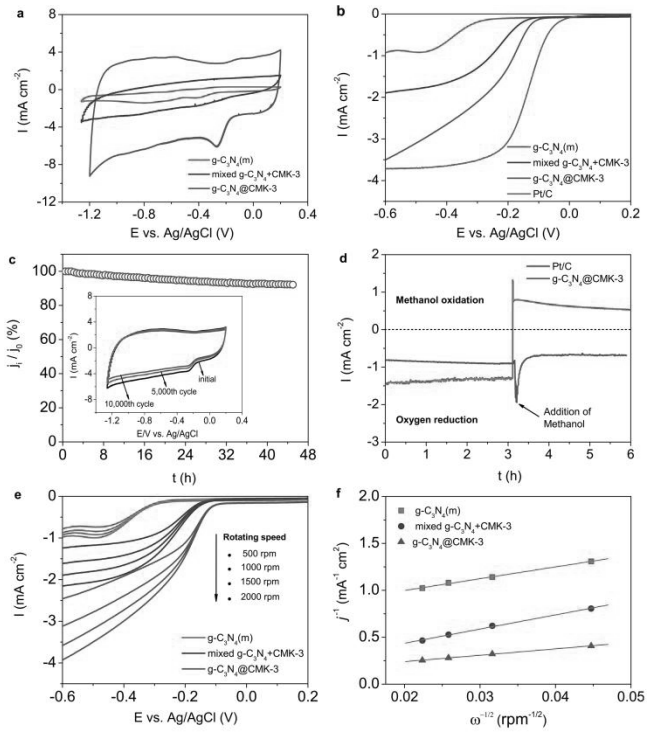

Figure 3. (a) Cyclic voltammograms of ORR on various electrocatalysts in O_2-saturated 0.1 M KOH solution. (b) LSV of various electrocatalysts on RDE at 1500 rpm in O_2-saturated 0.1 M KOH solution. (c) Current-time (i-t) chronoamperometric response of g-C_3N_4@CMK-3 at -0.3 V; inset represents cyclic voltammograms under continuous potentiodynamic sweeps. (d) Chronoamperometric responses of Pt/C and g-C_3N_4@CMK-3 at -0.3 V in O_2-saturated 0.1 M KOH solution without methanol (0-3 h) and with adding methanol (3-6 h). (e,f) LSV of various electrocatalysts on RDE at different rotating rate (500 to 2000 rpm) and corresponding Koutecky-Levich plots at -0.6 V.

The durability of g-C_3N_4@CMK-3 is evaluated by the chronoamperometric response under a constant cathodic voltage of -0.3 V. As shown in Figure 2c, the newly developed catalyst exhibited high stability with a very slow attenuation after 45 hours, and a high relative current of 92.2% still persisted. The CVs (inset in Figure 2c) also reveal the reliable stability of g-C_3N_4@CMK-3 with less than 10% cathodic current loss during ~10,000 continuous potential cycling. This excellent stability benefits from homogenous interactions of the g-C_3N_4 catalyst and CMK-3 support.

The methanol tolerance ability is an important issue for cathode materials in low-temperature fuel cells and also an obvious shortage of Pt-based catalysts. Remarkably, as shown in Figure 2d, the original cathodic ORR current of g-C_3N_4@CMK-3 under -0.3 V did not show significant change after the scheduled sequential addition of methanol into the electrolyte solution (the resulting methanol concentration is 3 M), suggesting that its original ORR performance was not affected by the addition of methanol. In comparison, the corresponding current on commercial Pt/C shifted from a cathodic current to a reversed anodic current in a very short time after the addition of methanol, indicating a conversion of dominated oxygen reduction to the methanol oxidation reaction, i.e., a poisoning of the catalyst. These results indicate that g-C_3N_4@CMK-3 is an ideal cathode catalyst for a direct methanol alkaline fuel cell.

A more detailed study of the RDE system at different rotating speeds was carried out to further investigate electrode's electrocatalytic ORR mechanisms and dominated processes (Figure 2e). Calculated from the slope of the Koutecky-Levich plots (Figure 2f), the number of electrons transferred per O_2 molecule (n) for ORR is 2.6, 1.7, and 4.0 for g-C_3N_4(m), mixed g-C_3N_4+CMK-3, and g-C_3N_4@CMK-3, respectively. It is clear that the typical ORR process on g-C_3N_4(m) is a combined pathway of $2e^-$ and $4e^-$ reductions. In contrast, g-C_3N_4@CMK-3 shows a perfect selectivity (nearly 100 %) with a more efficient $4e^-$ dominated ORR process. To the best of our knowledge, this is the first report on metal-free electrocatalysts showing such excellent ORR catalytic efficiency.

The n value on g-C_3N_4@CMK-3 is larger than that on Pt/C (n=3.8), indicating its higher catalytic efficiency for ORR. Furthermore, the g-C_3N_4@CMK-3 reveals a calculated kinetic-limiting current density (J_k) value of 11.3 mA cm^{-2} at -0.6 V, much higher than those on g-C_3N_4(m) (1.7 mA cm^{-2}) and the mixed g-C_3N_4+CMK-3 (8.7 mA cm^{-2}), and comparable with that on Pt/C (11.3 mA cm^{-2}) at the same cathodic voltage and mass of catalyst. The large J_k value on g-C_3N_4@CMK-3 displays its excellent catalytic activity for ORR. This optimized ORR performance on g-C_3N_4@CMK-3 can be attributed to the participation of CMK-3 mesoporous carbon framework, which not only serves as the support for homogenously-distributed and well-confined g-C_3N_4 catalyst, but also significantly improves the electron accumulation on the surface of g-C_3N_4 catalyst then enhancing the electron transfer efficiency in ORR.

Conclusions

We synthesized mesoporous g-C_3N_4@CMK-3 nanorods as a metal-free, facile-synthesis and low-cost ORR electrocatalyst, which exhibited a competitive electrochemical performance with commercial Pt/C including extremely high electrocatalytic activity and efficiency. The excellent ORR performance and reliable stability of g-C_3N_4@CMK-3 indicate that this new catalyst is a promising candidate for the next generation of highly efficient ORR electrocatalysts particularly for methanol alkaline fuel cells. The results further open up new avenues for achieving a wide variety of cheap and commonly available metal-free catalysts for broad applications across the areas of heterogeneous catalysis, sensor, photonic-catalysis, hydrogen production and lithium ion batteries.

Acknowledgement. This work was financially supported by the Australian Research Council (ARC) through the Discovery Project program (DP1095861, DP0987969).

References

1 Wang, X.; Maede, K.; Thomas, A.; Takanabe, K.; Xin, G.; Carsson, J. M.; Domen, K.; Antonietti, M. *Nat. Mater.* 2009, 8, 76.

2 Wang, Y.; Yao, J.; Li, H.; Su, D.; Antonietti, M. *J. Am. Chem. Soc.* 2011, 133, 2362.

3 Yang, S.; Feng, X.; Wang, X; Müllen, K. *Angew. Chem. Int. Ed.* 2011, 50, 5339.

4 Zheng, Y.; Jiao, Y; Chen, Liu, J.; Du, A.; Zhang, W., Zhu, Z.; Smith, S.; Jaroniec, M; Lu, G.; Qiao, S.Z., *J. Am. Chem. Soc.* 2011, 133, accepted.

5 Yang, W.; Fellinger, T; Antonietti, M. *J. Am. Chem. Soc.* 2011, 133, 206.

6. Liu, R.; Malotki, C.; Arnold, L.; Koshino, N.; Higashimura, H.; Baumgarten, M.; Müllen, K. *J. Am. Chem. Soc.* 2011, 133, 10372.